

Classification of CMIP5 Future Climate Responses by the Tropical Sea Surface Temperature Changes

Ryo Mizuta¹, Osamu Arakawa², Tomoaki Ose¹, Shoji Kusunoki¹, Hirokazu Endo¹, and Akio Kitoh²

¹Meteorological Research Institute, Tsukuba, Japan

²University of Tsukuba, Tsukuba, Japan

Abstract

Climate changes for the end of the 21st century projected by Coupled Model Intercomparison Project phase 5 (CMIP5) models are classified into three clusters by a cluster analysis of annual-mean tropical sea surface temperature (SST) change patterns. The classified SST change patterns are featured by the zonal gradient of the change in the equatorial Pacific and inter-hemispheric contrast of the warming. Precipitation and atmospheric circulation responses are composited for the clusters, and their relationships to the SST changes are examined. Precipitation increase is larger where SST warming is larger than surroundings and vice versa. Common precipitation and atmospheric circulation responses for each cluster are found also over tropical lands and the extratropics as well as in the tropical oceans, suggesting that some remote effects of the tropical SST change patterns could be one reason for less agreement among CMIP5 models in climate changes.

(Citation: Mizuta, R., O. Arakawa, T. Ose, S. Kusunoki H. Endo, and A. Kitoh, 2014: Classification of CMIP5 future climate responses by the tropical sea surface temperature changes. *SOLA*, 10, 167–171, doi:10.2151/sola.2014-035).

1. Introduction

Based on the Coupled Model Intercomparison Project phase 5 (CMIP5; Taylor et al. 2012) models projections, the future changes in surface air temperature and sea surface temperature (SST) for the end of the 21st century are not spatially uniform and also not seasonally constant (Collins et al. 2013). For the tropical ocean surface temperature, the strongest warming is projected on the equator and in the Northern Hemisphere subtropical regions.

Precipitation change also varies in space. While models show that global precipitation will increase with increased global mean surface temperature, changes in average precipitation in a warmer world exhibit substantial spatial variation (Collins et al. 2013). The spatial distribution of tropical precipitation changes will depend on the current precipitation climatology and also on future SST warming pattern (Christensen et al. 2013). The first effect is to increase precipitation near the currently rainy regions (“wet-get-wetter” effect; Held and Soden 2006; Chou et al. 2009), and the second effect is to increase precipitation where warming of SST exceeds the tropical mean and vice versa (“warmer-get-wetter” mechanism; Xie et al. 2010; Chadwick et al. 2013; Ma and Xie 2013).

Tropical SST changes vary among the models. Variances of SST change patterns in the CMIP5 models are large as well as in the CMIP3 models, in particular for zonal SST gradient changes along the equatorial Pacific (Christensen et al. 2013). This is related to the variance of mean precipitation and tropical circulation change through the effect mentioned above, which affect the extratropics, mainly through the changes in the teleconnection patterns from the tropics and changes in tropical cyclone genesis.

This study investigates how the inter-model difference of the tropical SST changes for the end of 21st century is related to that

of the precipitation and circulation changes. Horizontal patterns of the tropical SST changes projected by the CMIP5 models are classified using a cluster analysis method, and associated changes in the precipitation and circulation for each cluster are investigated. These analyses will give some information on what part of the uncertainty in the projected regional climate change could be attributed to the uncertainty of the tropical SST change. The classified SST change patterns can be used as the lower boundary change for atmospheric models to study on what part of the climate change could depend solely on the pattern of the SST change. We show a cluster analysis method and its results in Section 2. Composites of climate changes for the three SST clusters of the CMIP5 models will be given in Section 3. Summary and some remarks will be made in Section 4.

2. Cluster analysis of CMIP5 SST

The names of the CMIP5 models used in this analysis are listed in Table S1 in the auxiliary material. We used 28 model results from CMIP5 for which the historical, RCP2.6, RCP4.5, and RCP8.5 scenario experiments are available. Only one member is used even if the model has multiple experiments with different initial conditions. Cluster analysis is made for the SST difference between the historical and RCP8.5 experiments. This classification is used for other scenarios. Additionally, as we obtained 22 out of the 28 models for the RCP6.0 scenario experiments, we also made analysis for the 22 RCP6.0 experiments.

We use the same cluster analysis method as Murakami et al. (2012) and Endo et al. (2012), which was applied to the CMIP3 SRES A1B scenario runs. The detailed procedure for the cluster analysis is as follows: (1) for each of the 28 CMIP5 models, the annual-mean SST change from the present-day (1979–2003 of historical experiment) to the end of the 21st century (2075–2099 of RCP8.5 experiment) is computed; (2) the computed mean SST change is normalized by the tropical (30°S–30°N) mean SST change; (3) the multi-model ensemble mean of the normalized change is subtracted from that for each model experiment; (4) then, the inter-model pattern correlation r over the tropics (30°S–30°N) is computed between each pair of the models; and (5) norms (or distances) are defined as $2 \times (1 - r)$ for every pair, and the cluster analysis is performed using these norms. A small distance between two models indicates they share similar spatial patterns in the tropical SST change. Clustering is based on the single-linkage (or minimum-distance) method (e.g., Wilks 2011), in which the smallest distance between two models (or groups) is joined step-by-step. The clustering procedure is terminated when the final three groups are obtained. The effect of the mid-latitude ocean to the atmosphere is smaller, and there could be other classifications of the models in the north and south polar regions. Therefore, we use the SST only in the tropics to focus on the effect of the tropical ocean.

Figure S1 in the auxiliary material shows the normalized SST changes of all 28 models between the 1979–2003 mean of the historical experiment and the 2075–2099 mean of the RCP8.5 experiment. For each model, SST was normalized by the tropical (30°S–30°N) mean SST change, and then multiplied by the tropical SST change averaged for the total 28 models (2.74K). Figure 1 shows the dendrogram of the cluster analysis. It is noted that models from the same institute have a smaller distance than other

models, and thus tend to be clustered earlier. This characteristic has been also found in the cluster analysis of CMIP5 model climatology of surface temperature and precipitation (Knutti et al. 2013). As we ended up as three clusters, 8, 14, and 6 models are classified as Cluster 1, Cluster 2, and Cluster 3, respectively.

Based on the result of the cluster analysis above, we composed three kinds of the future SST change by averaging each cluster of the models, after normalized by the annual-mean tropical mean (30°S–30°N) SST change. Figure 2 shows the annual-mean normalized SST change between the present-day and the end of 21st century, for the composite of the total 28 models and the composites of the three clusters of the models, together with the deviations for each cluster from the total mean. The SST changes are multiplied by the annual-mean tropical SST change averaged for the total 28 models (2.74K) in order that the annual-mean tropical SST change becomes the same value as that in the 28 CMIP5 model mean. Note that the resultant three kinds of the SST change pattern have almost the same values of SST for not only the tropical mean but also the global mean. It is shown that SST warming even in the total mean is spatially inhomogeneous (Fig. 2a): warming is larger in the Northern Hemisphere than in the Southern Hemisphere, and the largest SST warming occurs in the northern North Pacific. Relatively larger warming is found in

the central and eastern tropical Pacific. This spatial pattern in the tropics is emphasized in Cluster 2 (Figs. 2c, f). The pattern in Fig. 2f is similar to the observed interannual variation pattern associated with ENSO, consistent with the CMIP3 result that projects El Niño-like response in many models (Yamaguchi and Noda 2006). In contrast, Cluster 1 (Figs. 2b, e) shows smaller warming in the eastern tropical Pacific, which is an opposite characteristic to Cluster 2. In addition, warming in the Southern Hemisphere is larger in Cluster 1, to the extent that the warming in the mid-latitudes (~40°) is about the same between the both hemispheres. Cluster 3 (Figs. 2d, g) has large warming in the western North Pacific. Warming is larger than the other clusters also around northern Indian Ocean and the North Atlantic. In contrast, warming in the Southern Hemisphere is smallest, thus the inter-hemispheric contrast is large.

More specifically, the clustered SST change patterns are featured by the zonal gradient of the change in the equatorial Pacific and inter-hemispheric contrast of the warming. Figure 3 shows the scatter diagram of the annual-mean normalized SST change of each model, for the difference between 15°S–30°S and 15°N–30°N versus the difference between 5°S–5°N, 150°W–90°W (called Niño 3 region) and 0°N–15°N, 130°E–150°E (called Niño West region)

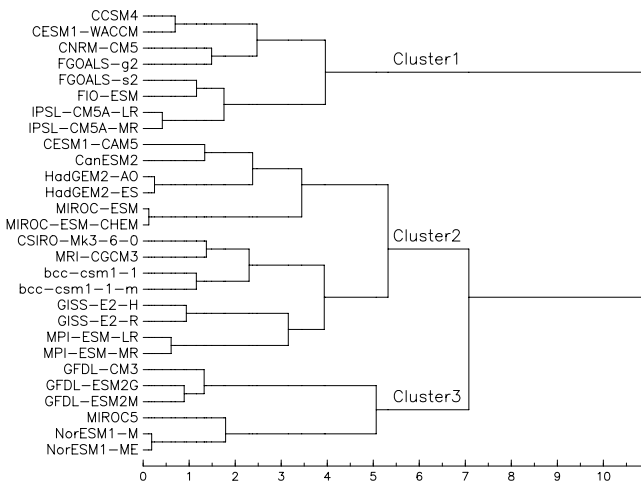


Fig. 1. Dendrogram of SST cluster analysis based on 28 CMIP5 SST changes in the tropics (30°S–30°N).

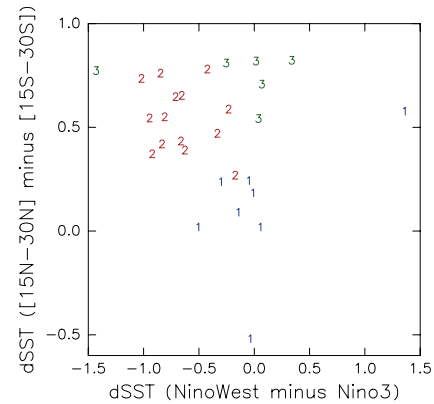


Fig. 3. Scatter diagram of the annual-mean SST change (K) of each model, for the difference between 15°S–30°S and 15°N–30°N versus the difference between 5°S–5°N, 150°W–90°W (called Niño 3 region) and 0°N–15°N, 130°E–150°E (called Niño West region). The change is normalized by the tropical mean for each model and then multiplied by 28 models mean tropical SST change (2.74K). The digits denote the cluster number of the models.

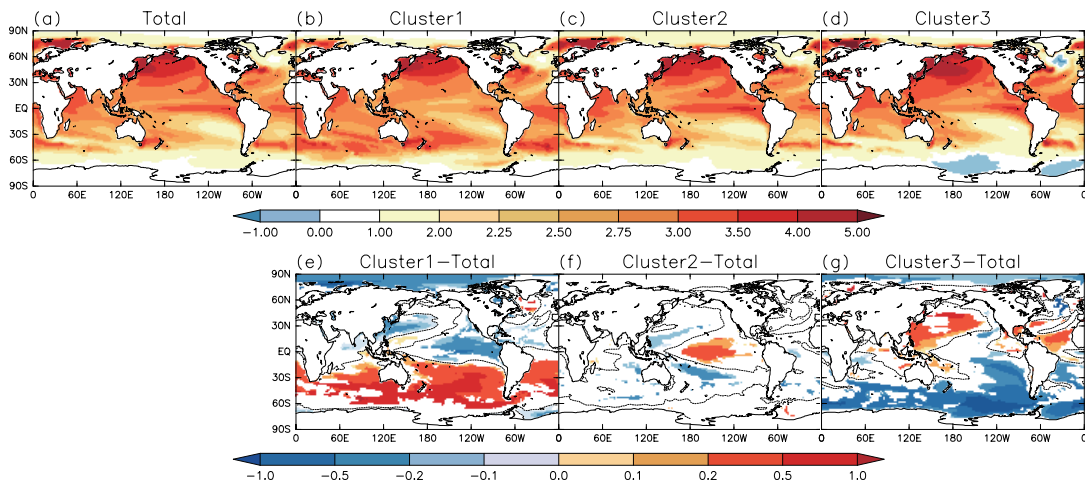


Fig. 2. Annual-mean sea surface temperature changes (K) from the present-day (1979–2003, historical experiment) and the end of the 21st century (2075–2099, RCP 8.5 experiment), for (a) the composite of total 28 models, and (b–d) the composites of the three clusters of the models. (e–g) Differences for each cluster from the total mean. The regions where over 75% of the models agree with the sign of the difference are colored. Contours denote 0. The change is normalized by the tropical (30°S–30°N) mean for each model before making composition, and then multiplied by 28 models mean tropical SST change (2.74K).

region). The three clusters are separated clearly, although there are two exceptional models. Cluster 1 is characterized by the small zonal gradient change and the small (or negative) inter-hemispheric gradient change, Cluster 2 is characterized by the large zonal gradient decrease and the modest inter-hemispheric contrast, and Cluster 3 is characterized by the small zonal gradient change and the large inter-hemispheric contrast.

The composites of the annual-mean normalized SST change for the three clusters have been made also for the other RCP experiments. The pattern correlation coefficients between the different experiments are shown in Table 1 (top right). In any clusters, pattern correlation between the changes for the RCP2.6 and those for the other RCP experiments are commonly lower than the other pairs. Since amplitudes of the changes from the historical to the RCP2.6 experiments are so small, internal decadal variability or the effects of aerosol changes could be comparable to the effects of CO₂ increase, and the ratio of warming over land to that over ocean could be different from the other scenarios. While there are some exceptions for the Cluster 1, the correlation coefficients are over 0.9 in most of the pairs. This suggests that the annual-mean normalized SST changes could be treated as the same to a large extent among the four RCP scenarios. If the normalized SST changes are the same among the scenarios, we have possibility of applying “pattern scaling” (e.g., Mitchell et al. 1999) to obtain many future changes from one experiment just by multiplying the amplitude of the change.

3. Composites of climate changes for the three SST clusters of the CMIP5 models

Tropical SST distribution has large impacts not only on in situ precipitation but also on various remote responses in precipitation and atmospheric fields. In this section, composites of climate

changes for the three clusters of the CMIP5 models are shown in terms of precipitation and sea-level pressure (SLP). The change for each model is interpolated to 2.5-degree grid and normalized by the tropical mean SST change before making the composition.

Figure 4 shows the changes in annual-mean precipitation between the present-day (1979–2003, historical experiment) and the end of the 21st century (2075–2099, RCP 8.5 experiment) composited for the total 28 models and the three clusters of the models. The December-January-February (DJF) mean and the June-July-August (JJA) mean are also shown in Figs. S2 and S3 in the auxiliary material, respectively. While it is common to the all clusters that the precipitation increases in the tropics and extratropics, and decreases in the subtropics, there are systematic differences between the clusters in precipitation changes over the tropics, associated with the differences in the SST changes.

In the total mean (Fig. 4a), precipitation increases more over the central equatorial Pacific and less over the western equatorial Pacific. Moreover, decrease is found in the western part of the maritime continent. This is associated with the El Niño-like SST response pattern shown in Fig. 2a. The decrease is conspicuous in the JJA mean (Fig. S3c). These characteristics are more conspicuous in Cluster 2 (Fig. 4c, f). In Cluster 1 and 3, more increase than Cluster 2 is found from the maritime continent to the South Pacific Convergence Zone (SPCZ) region, which is opposite sign from Cluster 2. In contrast, precipitation increase over the central and eastern equatorial Pacific is less than Cluster 2 (Fig. 4b, d, e, g). This is associated with the less SST warming in this region. Precipitation is increasing over Amazon and the central Africa in Cluster 1 (Fig. 4b), although decreasing in the other clusters. These characteristics are seen also in the DJF mean (Fig. S2b, e) and the JJA mean (Fig. S3b, e). Cluster 3 is characterized by the larger decrease over the subtropics of the Southern Hemisphere (Fig. 4d, g). This would be related to the less SST warming in eastern South Pacific (Fig. 2g). Over the Asian monsoon region,

Table 1. The pattern correlation coefficients of (top right) annual-mean normalized SST change and (bottom left) annual-mean normalized precipitation change between the four RCP experiments for the composites of the three clusters. The values over 0.9, 0.8, and below 0.8 are colored by red, green, and blue, respectively.

Cluster1	RCP2.6	RCP4.5	RCP6.0	RCP8.5	Cluster2	RCP2.6	RCP4.5	RCP6.0	RCP8.5	Cluster3	RCP2.6	RCP4.5	RCP6.0	RCP8.5
RCP2.6		0.93	0.91	0.76	RCP2.6		0.96	0.94	0.91	RCP2.6		0.96	0.95	0.92
RCP4.5	0.83		0.93	0.93	RCP4.5	0.93		0.99	0.98	RCP4.5	0.79		0.99	0.98
RCP6.0	0.71	0.86		0.82	RCP6.0	0.91	0.96		0.98	RCP6.0	0.74	0.95		0.99
RCP8.5	0.73	0.94	0.84		RCP8.5	0.90	0.96	0.96		RCP8.5	0.70	0.94	0.96	

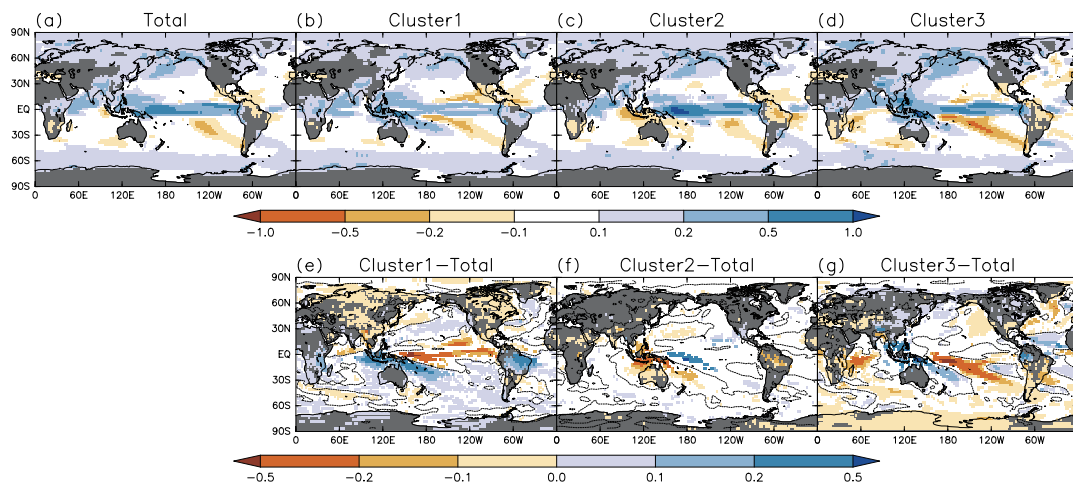


Fig. 4. Annual-mean normalized precipitation changes ($\text{mm day}^{-1} \text{K}^{-1}$) from the present-day (1979–2003, historical experiment) and the end of the 21st century (2075–2099, RCP 8.5 experiment), for (a) the composite of total 28 models, and (b–d) the composites of the three clusters of the models. (e–g) Differences for each cluster from the total mean. The regions where over 75% of the models agree with the sign of the difference are colored. Contours denote 0. The change for each model is interpolated to 2.5-degree grid and normalized by the tropical mean SST change before making the composition.

increase of precipitation is larger in Cluster 3, especially around Indochina and the Philippines, associated with the larger SST warming over the western North Pacific (Fig. 2g). This is clearer in the JJA mean (Fig. S3e, g). Over the Caribbean Sea and subtropical North Atlantic, in contrast, decrease of precipitation is smaller in Cluster 3.

The pattern correlation coefficients of the normalized precipitation change between the different experiments are shown in Table 1 (bottom left). Except for the RCP2.6 experiment, the correlation coefficients are over 0.8 in all of the pairs, even though the cluster analysis has been made for the SST change. It is noted that, in Cluster 1, correlation between the RCP6.0 and the others are relatively lower, partly because 4 models out of 8 are unavailable for RCP6.0 in Cluster 1 (Table S1).

Figure 5 shows the same future changes as Fig. 4, but for the annual-mean SLP. The DJF mean and the JJA mean are also shown in Figs. S4 and S5 in the auxiliary material, respectively. Mean sea-level pressure responses for the total 28 models (Fig. 5a) are projected to decrease in high latitudes and increase in the mid-latitudes with poleward shifts of the mid-latitude jets (Collins et al. 2013). Over the maritime continent, increase of SLP is larger than surroundings, leading to the reduction of zonal SLP gradient over the tropical Pacific. Cluster 2 has a similar characteristic to the total mean (Fig. 5c) and a small difference from the total mean (Fig. 5f). Cluster 1 has a smaller increase than the other clusters (Fig. 5b, e), associated with the larger increase of precipitation over this region. This anomaly in SLP is extending to the subtropics around Australia and south of Japan (Fig. 5e). A relatively larger SLP increase is seen over the Eurasian continent in winter (Fig. S4e). In Cluster 3, SLP is increasing larger in the central equatorial Pacific (Fig. 5d, g) and decreasing in the Northern continents. The increase of SLP is larger also over mid-latitudes of the Pacific and the Atlantic. This is clear in the Northern Hemisphere in DJF (Fig. S4g) and in the Southern Hemisphere in JJA (Fig. S5g), suggesting that a difference in the change of the wintertime storm track activity in mid-latitudes. In JJA, larger increase of SLP is found over the Indian Ocean. This would contribute to an enhancement of the eastward moisture transport in the Asian summer monsoon, consistent with the larger increase of the Asian monsoon precipitation in Cluster 3 (Fig. S3g). The JJA situation of Cluster 1 (Fig. S3e) is reverse to that of Cluster 3.

The DJF and JJA mean surface temperature changes are shown in Figs. S6 and S7 in the auxiliary material. The warming is relatively smaller/larger over the Northern continents in Cluster 1/Cluster 3 (Figs. S6e, g, S7e, g), consistent with the SLP changes. In addition, associated with the El Niño-like/La Niña-like SST response pattern shown in Fig. 2e/2f, the decrease of cold surge over the East Asia is enhanced/suppressed, also consistent with the SLP changes around south of Japan (Fig. S4e).

4. Summary and concluding remarks

This paper focused on the classification of climate changes for the end of the 21st century projected by CMIP5 models using a cluster analysis of annual-mean tropical SST change patterns. The classified SST change patterns are characterized by the zonal gradient of the change in the equatorial Pacific and inter-hemispheric contrast of the warming. Associated with different tropical SST changes among the clusters, characteristic precipitation and atmospheric circulation responses are found in each cluster. The relationship between the different SST changes and the different precipitation responses among the clusters seems to follow the “warmer-get-wetter” mechanism mentioned in the Introduction. The precipitation and atmospheric circulation response are found also over the tropical lands and the extratropics as well as in the tropical oceans, suggesting that some remote effects could be one reason for less agreement among CMIP5 models in climate changes. It is noted that it should be taken into consideration that, due to the insufficient model number, there could exist high-latitude surface differences between the clusters (in sea ice and/or land surface) unrelated to the tropics, which affect extratropical atmosphere.

The obtained SST changes as shown in Fig. 2b, c, d can be used as the lower boundary change for atmospheric models to study on what part of the climate change could depend solely on the pattern of the SST change. In particular, the use of high-resolution atmospheric models can give us information on smaller-scale extreme events than CMIP5 coupled models themselves. We can cover the range of inter-model spread with smaller number of experiments than giving every change pattern from all CMIP5 models. Murakami et al. (2012) showed that regional future projections of frequency of tropical cyclones are depending on the SST change pattern. Endo et al. (2012) showed that the uncertainty of future projections in extreme precipitation over Asia is large and comes from the SST change pattern as well as physical parameterization schemes of the model. We are now doing ensemble projections using the SST change patterns obtained in this study, with a higher-resolution atmospheric model and even higher-resolution regional downscaling from it. These experiments would enable us to discuss more on the uncertainty of the future projections of smaller-scale and/or extreme phenomena.

Acknowledgments

We acknowledge the modeling groups, the Program for Climate Model Diagnosis and Intercomparison (PCMDI) and the WCRP's Working Group on Coupled Modeling (WGCM) for their

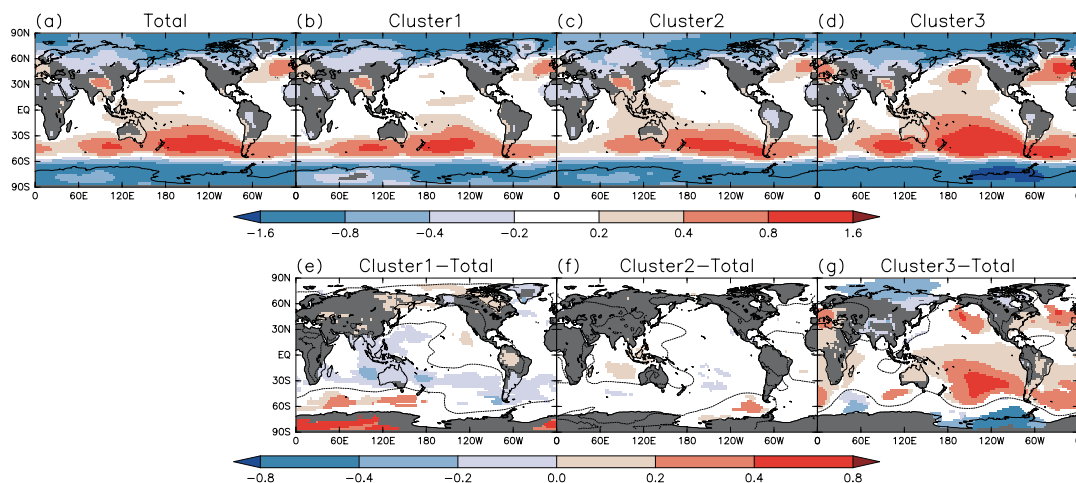


Fig. 5. As for Fig. 4, but for annual-mean normalized sea-level pressure changes (hPa K^{-1}).

roles in making available the WCRP CMIP5 multi-model datasets. This study was supported by the SOUSEI Program of the Ministry of Education, Culture, Sports, Science, and Technology of Japan (MEXT), and the Environmental Research and Technology Development Fund (2A-1201) of the Ministry of Environment of Japan. We thank two anonymous reviewers for constructive comments.

Supplements

In the auxiliary material, list of CMIP5 models used is shown in Table S1. Annual mean SST changes for each model are shown in Fig. S1. DJF and JJA mean normalized precipitation changes are shown in Figs. S2 and S3. DJF and JJA mean normalized SLP changes are shown in Figs. S4 and S5. DJF and JJA mean normalized surface temperature changes are shown in Figs. S6 and S7.

References

- Chadwick, R., I. Boutle, and G. Martin, 2013: Spatial patterns of precipitation change in CMIP5: Why the rich don't get richer in the tropics. *J. Climate*, **26**, 3803–3822, doi:10.1175/JCLI-D-12-00543.1.
- Chou, C., J. D. Neelin, C.-A. Chen, and J.-Y. Tu, 2009: Evaluating the “rich-get-richer” mechanism in tropical precipitation change under global warming. *J. Climate*, **22**, 1982–2005, doi:10.1175/2008JCLI2471.1.
- Christensen, J. H., K. Krishna Kumar, E. Aldrian, S.-I. An, I. F. A. Cavalcanti, M. de Castro, W. Dong, P. Goswami, A. Hall, J. K. Kanyanga, A. Kitoh, J. Kossin, N.-C. Lau, J. Renwick, D. Stephenson, S.-P. Xie, and T. Zhou, 2013: Climate phenomena and their relevance for future regional climate change, *Climate Change 2013: The Physical Science Basis. Working Group I Contribution to the Fifth Assessment Report of the Intergovernmental Panel on Climate Change*, T. F. Stocker, D. Qin, G.-K. Plattner, M. Tignor, S. K. Allen, J. Boschung, A. Nauels, Y. Xia, V. Bex and P. M. Midgley, Eds., Cambridge University Press, Cambridge, United Kingdom and New York, NY, USA., 1217–1308.
- Collins, M., R. Knutti, J. Arblaster, J.-L. Dufresne, T. Fichet, P. Friedlingstein, X. Gao, W. J. Gutowski, T. Johns, G. Krinner, M. Shongwe, C. Tebaldi, A. J. Weaver, and M. Wehner, 2013: Long-term climate change: projections, commitments and irreversibility, *Climate Change 2013: The Physical Science Basis. Working Group I Contribution to the Fifth Assessment Report of the Intergovernmental Panel on Climate Change*, T. F. Stocker, D. Qin, G.-K. Plattner, M. Tignor, S. K. Allen, J. Boschung, A. Nauels, Y. Xia, V. Bex and P. M. Midgley, Eds., Cambridge University Press, Cambridge, United Kingdom and New York, NY, USA, 1029–1136.
- Endo, H., A. Kitoh, T. Ose, R. Mizuta, and S. Kusunoki, 2012: Future changes and uncertainties in Asian precipitation simulated by multiphysics and multi-sea surface temperature ensemble experiments with high-resolution Meteorological Research Institute atmospheric general circulation models (MRI-AGCMs). *J. Geophys. Res.*, **117**, D16118, doi:10.1029/2012JD017874.
- Held, I. M., and B. J. Soden, 2006: Robust response of the hydrological cycle to global warming. *J. Climate*, **19**, 5686–5699, doi:10.1175/JCLI3990.1.
- Knutti, R., D. Masson, and A. Gettelman, 2013: Climate model genealogy: Generation CMIP5 and how we got there. *Geophys. Res. Lett.*, **40**, 1194–1199, doi:10.1002/grl.50256.
- Ma, J., and S.-P. Xie, 2013: Regional patterns of sea surface temperature change: a source of uncertainty in future projections of precipitation and atmospheric circulation. *J. Climate*, **26**, 2482–2501, doi:10.1175/JCLI-D-12-00283.1.
- Mitchell, J. F. B., T. C. Johns, M. Eagles, W. J. Ingram, and R. A. Davis, 1999: Towards the construction of climate change scenarios. *Clim. Change*, **41**, 547–581, doi:10.1023/A:1005466909820.
- Murakami, H., R. Mizuta, and E. Shindo, 2012: Future changes in tropical cyclone activity projected by multi-physics and multi-SST ensemble experiments using the 60 km-mesh MRI-AGCM. *Clim. Dyn.*, **39**, 2569–2584, doi:10.1007/s00382-011-1223-x.
- Taylor, K. E., R. J. Stouffer, and G. A. Meehl, 2012: An overview of CMIP5 and the experiment design. *Bull. Amer. Meteor. Soc.*, **93**, 485–498, doi:10.1175/bams-d-11-00094.1.
- Wilks, D. S., 2011: *Statistical Methods in the Atmospheric Sciences*, 3rd ed. Academic, Oxford, U.K., 704pp.
- Xie, S. P., C. Deser, G. A. Vecchi, J. Ma, H. Teng, and A. T. Wittenberg, 2010: Global warming pattern formation: Sea surface temperature and rainfall. *J. Climate*, **23**, 966–986, doi:10.1175/2009JCLI3329.1.
- Yamaguchi, K., and A. Noda, 2006: Global warming patterns over the North Pacific: ENSO versus AO. *J. Meteor. Soc. Japan*, **84**, 221–241, doi:10.2151/jmsj.84.221.

Manuscript received 22 July 2014, accepted 12 September 2014
SOLA: <https://www.jstage.jst.go.jp/browse/sola/>